AFM lithography for the definition of nanometer scale gaps: application to the fabrication of a cantilever based sensor with electrochemical current detection.

María Villarroya[1], Francesc Pérez-Murano[2], Cristina Martín[2], Zachary Davis[3], Anja Boisen[3], Jaume Esteve[2], Eduard Figueras[2], Josep Montserrat[2], Núria Barniol[1].

1 Dept. Enginyeria Electrònica. Univ. Autònoma de Barcelona. 08193 Bellaterra. Spain

PHONE: +34 93 581.35.14. FAX: +34 93 581.26.00. e-mail: Maria.Villarroya@uab.es

2 Institut de Microelectrònica de Barcelona (IMB-CNM). CSIC. Campus UAB. 08193 Bellaterra. Spain. PHONE: +34 93 594.77.00. FAX: +34 93 580.14.96

3 Mikroelektronik Centret. Danmarks Tekniske Universitet, Bldg 345, 2800 Lyngby. Denmark. PHONE: +45 4525.5700. FAX: +45 4588.7762

e-mail: Maria.Villarroya@uab.es

http://einstein.uab.es/ecas

Abstract

The concept, design and fabrication of a cantilever-based sensor operating in liquid for biochemical applications are reported. A novel approach for detecting the deflection of a functionalized cantilever is proposed. It consists on detecting the change of the electrochemical current level when a voltage is applied between a deflecting cantilever, acting as one of the electrodes, and a reference fixed electrode placed in close proximity to the free extreme of the cantilever. The detection is possible since the distance between both electrodes is smaller than 50 nm. The sensor is fabricated by using a combination of MEMS technology and AFM-based lithography.

1. Introduction

Miniaturization of biochemical sensors allows to improve their sensitivity and integration potential. During the last years, different kinds of micro/nano biochemical sensors have been proposed. Some of them take advantage of new emerging nanofabrication methods that provide the technical capability to fabricate new kind of devices. Particularly, cantilever based sensors (CBS) have been proposed as very sensitive detectors for heat, surface stress, mass, chemical and biochemical recognition [1-4]. CBS are based on detecting the change of the deflection or, for dynamic or resonating mode, the change of resonance frequency of a micro/nano fabricated cantilever due to the effect of an external magnitude. For biochemical detection, the surface of the cantilever is functionalized to allow the detection of specific molecules. The interest of developing CBS is based on the simplicity of the design and fabrication, its compatibility with CMOS technology [5,6] and its flexibility to operate in different environments.

Most of the examples of CBS proposed until now are based on the optical detection of the cantilever deflection by means of an external set-up consisting of a laser and a photodiode. In consequence, miniaturization of such a system is limited. Proposed alternatives to optical detection are capacitive detection [7], piezoresistive detection [8] or piezoelectric detection [9]. However, these alternatives present several difficulties: impossibility for operation in liquid (capacitive detection), or limitations for being miniaturized towards submicron dimensions (piezoresistive and piezoelectric). Here, we propose a new method to detect the deflection of the cantilever for operation in liquid.

The bending of the cantilever is detected by the variation of the electrochemical current between two closely positioned electrodes. This sensing method allows the detection to be done in liquid, providing the natural environment for biological sensors. Moreover, detection of the deflection by means of acquiring electrical current is very easy to implement and fabricate, and it can be used to develop sensors based on arrays of cantilevers for multiple specific detection or for differential detection.

2. Principle and design of the sensor

The detection of the cantilever deflection is performed by measuring the change of electrochemical current between the mobile cantilever and another fixed electrode placed at the free extreme of the cantilever. To assure that the change of the electrochemical current will be as large as possible and detectable compared to the faradaic current through all the lateral area of the cantilever, the change of electrochemical conduction has to be restricted to a fixed, small area. In consequence, small fingers are defined at the free end of the cantilever as active electrodes (Figure 1). When the cantilever deflects as a consequence of detecting specific molecules, which induce surface stress on the cantilever surface, a change of the relative position between the electrodes takes place. This change provokes a variation of the electrochemical current detected, due to the fact that the electrochemical current is extremely sensitive to the effective facing cross-section between electrodes [10, 11]. Figure 2 shows a 3D-Schematic view of the sensor structure at rest (figure 2.a) and when bending due to either mass deposition or a chemical reaction (figure 2.b).

In order to validate the feasibility of the detection approach, preliminary tests with an electrochemical STM have been done. The set-up simulates the working conditions of the sensor: a microfabricated silicon tip is approached towards a silicon surface while the electrochemical current is acquired. Tip and surface are immersed in a biological compatible solution 1mM TRIS, 150mM NaCl i 40 mM ClMg (pH=7.4). The experiment reveals that the electrochemical current doubles every 10 nm when the tip-surface separation is less than 50 nm [12].

Cantilevers with different dimensions have been fabricated in order to obtain the appropriate values of the spring constant, k. It has been shown that cantilevers with spring constant values of around 20pN/nm allow the detection of DNA hybridation [4]. The dimensions of these cantilevers will be defined in order to i) match this value of the spring constant and ii) according to the technological constraints. The sensor is fabricated by micromachining technology using Silicon On Insulator (SOI) 4 inch wafers (bulk and SOI Silicon layers are p-type <100> and with 1.0 to 30.0 Ω·cm resistivity; bulk silicon layer are 525μm thick, the buried oxide 1000±50 nm and the SOI silicon layer 1,30±0,50 μm). In consequence, silicon is the structural layer of which the cantilever and the electrodes are made. The SOI layer has a nominal thickness of 1.3 μm that will determine the final thickness of the cantilever. Due to variations across the wafer of the thickness of the SOI layer, variation of the spring constant from one device to the other in the same wafer will occur. For this reason, a range of dimensions for the cantilevers have been defined. In table 1, data of the dimensions implemented are included.

At the free end of the cantilever, small electrodes (called finger-electrodes) are defined to minimize the distance between electrodes and to collect the electrochemical-current. These structures consist of small cantilevers with higher spring constant, so that they will not bend due to the surface stress that causes the cantilever bending.

Several structures have been designed. All the structures have been fabricated in the same wafer. The lateral width of the finger-electrodes is mainly determined by the combination of optical and AFM lithography. As the gap between electrodes has to be smaller than 100 nm, it will be defined by AFM nano-oxidation [13]. The area that the AFM microscope can pattern limits the maximum width of these finger-electrodes, which is defined by optical lithography. Figure 3 shows the implemented structures. The width of the finger-electrodes in figure 3.a) is 20 μm; in figure 3.b) is 5 μm and the separation is 5 μm. The design of figure 3.c) doubles the number of finger-electrodes with respect to figure 3.b).

3. Expected value of the electrochemical current

As a first approach, we can assume that the electrochemical current that will be measured follows Ohm's law:

$$I = \frac{V}{R} \qquad (1)$$

where V is the voltage between the cantilever and the electrodes, and R is the electrolytic resistance :

$$R = \rho \frac{l}{A} \qquad (2)$$

where ρ is the specific resistance of the medium, l is the distance between electrodes and A is the effective cross-section of the face to face electrodes.

We consider a linear bending of the cantilever. Assuming that the force that will provoke the bending of the cantilever is 300 pN [4] and that the cantilever spring constant is of 20 pN/nm, the estimated bending at the free extreme of the cantilever is 15 nm. If, for example, we consider the case of a particular cantilever, with dimensions of 500 μm length, 1.3μm thick and 25 μm width, and with 4 fingers (figure 3.b) composing the structure at the end of the cantilever, the variation in effective area will be 0.29 μm^2, so that the total variation on the detected current will be around 4.5%. In this calculation, we have not taken into account the effect of the double layer, which will cause an additional change of the electrochemical current with distance [10] and that it may account for the larger change of current observed in the electrochemical STM experiments [12].

4. Fabrication process and results

The fabrication of the sensor is based on the combination of standard microfabrication processes with AFM lithography [13] on SOI substrates. The full process sequence consists of microfabrication processes except at the end when the AFM nanolithography is used to define the nanometer-scale gap between the cantilever and the reference electrode.

Microfabrication processes are used to define the microcantilever and the reference electrode. In this case, double-aligned optical lithography is used. First, a window is defined in the rear part of the wafer that will be later used for doing the back etching process. Then, the areas of the contact pads are defined by depositing a thick aluminum layer on the selected areas. Next, the cantilever, reference electrode and metal line areas are defined by a thin layer of aluminum that will serve as a mask for a RIE etching. A cavity (or reservoir) is created by etching in KOH from the backside of the wafer. This cavity will define the volume of liquid that will be used in the detection experiments and it will allow to obtain free-standing cantilevers. After this, the cantilevers and electrodes structures as well as the pads for external electrical contact are defined by reactive ion etching from the wafer front side. In figure 4, it is shown an SEM image of the cantilever and the cavity obtained from the back side of the wafer. Note that at this point, the gap between electrodes (cantilever and fix electrode) is not defined.

The process for the definition of the gap between electrodes is defined in Figure 5. The remaining thin aluminium layer from the microfabrication processing is first removed by chemical etching because it becomes fully oxidized after the RIE process. A new fresh 8 nm thick aluminium layer is deposit by DC magnetron sputtering on the front side as well as on the back side of the wafer. The aluminium layer on the back side of the wafer is necessary to avoid an overetching of silicon (figure 5a). Notice that at this point the cavities and the electrodes structures are completely defined. Next the AFM nanolithography step is realized (figure 5b). On each finger, a line across it is defined. Using AFM in dynamic mode, the aluminium is locally oxidized by drawing lines as long

as the finger width. As this nanolithography process is performed on the already micromechanized floating structures, the AFM is operated in the dynamic mode or tapping mode for imaging and oxidation in order to reduce as much as possible the interaction force between the AFM tip and the cantilever [14, 15]. The aluminium oxide grown during the AFM lithography is selectively removed (Figure 5c). Then, the pattern (line) is transferred to the underlying silicon by anisotropic RIE, which results in the creation of the gap (Figure 5d). Next step is to remove the aluminium layer to completely release the cantilever to the side finger electrodes (Figure 5e).

Figure 6 shows dynamic mode AFM images of the line defined on the surface of one of the finger electrodes after the AFM local oxidation process (figure 6a), and after the selective removal of the oxidized area (figure 6b). The AFM local oxidation is performed in air (60 % RH), using bare silicon tips and stiff cantilevers (spring constant k = 25 N/m). The voltage applied is 35 V (sample positive), the scanning speed is 0.3 μm/s and the oxidation is performed in non-contact mode to increase the life-time of the tip. The line profiles extracted from the AFM images show a depth of 9.5 nm after the aluminium oxide removal, indicating that in the line region, the aluminium has been totally removed. The relation between the height (4 nm) and depth of the line is consistent with the expected volume expansion of the aluminium oxide with respect to the aluminium, if the full thickness of the aluminium is oxidized at the region of the line. The different angle of the line as it appears in the AFM images is due to the fact that the sample was removed from the AFM stage for the etching process, so that the relative orientation between sample and scanning direction changed.

In the first prototype after a partial dry etching (not the full thickness of the SOI layer), a separation of 50 nm between electrodes has been achieved (Figures 7). Figure 8 are SEM images of the gap at one of the fingers electrodes realized after the full RIE process. In Figure 8a) the electrodes are still joined by the bottom aluminium layer on the back side of the structure. In figure 8b the electrodes are completely separated after pressing down with an AFM tip to break the aluminium layer. The different contrast of the images of figure 8 is due to the fact that they have been taken at different acceleration energies. It is clearly appreciated the two aluminium layers (which appear more transparent in figure 8a because of the higher energy of the electrons). The remaining silicon (darker area in figure 8b) is clearly over-etched, resulting in a smaller width of the finger electrodes and with a wider gap separation between electrodes. The smaller separation that has been achieved after the complete RIE process (over the 1.3 μm thick SOI layer) is of 350 nm. Currently, work is under progress to optimize the RIE process. Figure 8c shows an SEM image of the completely released structure. The fixed electrode is defocused with respect to the cantilever because after the creation of the gap, a steady state bending of the cantilever has arisen. The origin of this bending is thought to be caused by the surface stress induced by the aluminium layers or by a built-in stress of the SOI layers.

5. Mechanical characterization

AFM has been used to estimate the spring constant of the cantilever, after the creation of the gap. The cantilever was pressed down with the AFM tip (AFM cantilever spring constant of 25 N/m) near its free end. Figure 9a shows an optical image of the AFM tip on the cantilever surface while pressing down with the AFM operating in contact mode.

Figure 9b is an optical image of the same area but with the AFM tip separated from the cantilever. The bending of the AFM cantilever was measured by the laser detection system of the AFM and the bending of the fabricated cantilever was measured by the optical microscope of the AFM. The measurement was repeated at several locations on top of the cantilever, and finally the value of the spring constant of the fabricated cantilever was calculated to be of 17 ± 2 pN/nm.

This fabricated cantilever was designed to have a spring constant in the range between 20 pN/nm and 400 pN/nm, depending on the value of the thickness of the SOI layer at that specific location (the other dimensions were designed to be 100 μm for the width and 400 μm for the length). The value obtained experimentally is smaller than the theoretical one, but within the wanted range. The divergence from the estimated value is due to some variation in the process. On one hand the cantilever length (580 μm) is larger than the designed length, due to the larger size of the window overture. In addition, during the RIE process to separate the electrodes, the cantilever has been underetch laterally, thus the cantilever width (95 μm) has been reduced. These variations on the dimensions according with (1) explain that the actual value of the cantilever spring constant is lower than the expected.

6. Conclusions

A new approach for the detection of a cantilever deflection in a liquid environment has been presented. It is based on detecting the change of electrochemical current between

the deflecting cantilever and a fix electrode separated few nanometers. The design of the structure has taken into account the required sensitivity of the cantilever for biochemical detection and the maximization of the change of electrochemical current. The fabrication process requires the combination of standard surface and bulk silicon micromachining with AFM nanolithography. We have shown the technological viability of the approach by completing the fabrication of a first prototype. The simplicity of a deflection detection scheme based on current detection will allow in the future the integration of several sensors in the same chip to perform 'in situ' signal processing that will increase the sensitivity and performance of complete sensor systems.

Acknowledgments

This work has been partially funded by the projects NANOBIOTEC (CICYT-DPI2000-0703-C03) and NANOMASS II (EU-IST-2001-33068).

References

[1] R. Berger, Ch.Gerber, H. P. Lang, J.K.Gimzewski. Micromechanics : *A toolbox for Femtoscale Sience : « Towards a Laboratory on Tip ».* Microelectronic Engineering **35**, 373 (1997).

[2] O.Brand, H.Baltes. *Micromachined resonant sensors. An overview*. Sensors, vol.4, Willey-VCH, (1998).

[3] F.M.Battiston, J.P.Ramseyer, H.P.Lang, M.K.Baller, Ch.Gerber, J.K.Gimzewski, E.Meyer, H.J.Güntherodt. *A chemical sensor based on a microfabricated cantilever array with simultaneous resonance-frequency and bending readout*. Sensors and Actuators (B), **77**, 122-131 (2001).

[4] J.Fritz, M.K. Baller, H.P. Lang, H.Rothuizen, P.Vettiger, E. Meyer, H.-J. Güntherodt, Ch. Gerber, J. K. Gimzewki. *Translating Biomolecular Recognition into Nanomechanics*. Science. **288**, 316-318 (2000)

[5] Z.J. Davis, G. Abadal, B. Helbo, O. Hansen, F. Campabadal, F. Pérez-Murano, J. Esteve, E. Figueras, J. Verd, N. Barniol, A. Boisen. *Monolithic integration of mass sensing nano-cantilevers with CMOS circuitry.* Sensors and Actuators A **105,** 311–319, (2003).

[6] C. Hagleitner, A.Hierlemann, D. Lange, A. Kummer, N. Kernesss, O. Brand, H. Baltes. *Smart single-chip gas sensor microsystem*. Nature **414,** 293-296 (2001).

[7] Z.Davis, G.Abadal, E.Forsen, O.Hansen, F.Campabadal, E.Figueras, J.Esteve, J.Verd, F.Pérez-Murano, X.Borrisé, S.G.Nilsson, I.Maximov, L.Montelius, N.Barniol, A.Boisen. *Nanocantilever based mass sensor integrated with CMOS*

circuitry. Digest of Technical papers of The 12th International Conference on Solid-State Sensors, Actuators and Microsystems, Transducers'03. 496-499 (2003).

[8] X.Yu, J.Thaysen, O.Hansen, A.Boisen. *Optimization of sensitivity and noise in piezoresistive cantilevers.* Journal of Applied Physics, **92**, 6296-6301 (2002).

[9] T. Ito and T. Suga. *Development of a force sensor for atomic force microscopy using piezoelectric thin fims.* Nanotechnology, **4**, 218-224 (1993)

[10] A. J. Bard, P.R. Unwin, D.O. Wipf and F. Zhou. *Scanning Electrochemical Microscopy. Scanned Probe Microscopy*. AIP Conference Proceedings 241. (1992). Pages 235-247.

[11] M.-B. Song, J.-M- Jang, C.-W. Lee. *Electron Tunneling and Electrochemical Current through Interfacial Water Inside an STM Junction*. Bull. Korean Chem. Soc. **23** ,71-74 (2002)

[12] F. Pérez-Murano, I. Pérez, F. Sanz. *Private Communication.*

[13] Z.J.Davis, G.Abadal, O.Hansen, X.Borrisé, N.Barniol, F.Pérez-Murano, A.Boisen. *AFM lithography of aluminium for fabrication of nanomechanical systems*. Ultramicroscopy, **97,** 467-472 (2003).

[14] F. Pérez-Murano, G. Abadal, N. Barniol, J. Servat, P. Gorostiza, F. Sanz *Nanometer scale oxidation of silicon (100) surfaces with tapping mode AFM* J.Appl.Phys. **78**, 6797-6801 (1995)

[15] A. San Paulo and R. García; *Tip-surface forces, amplitude and energy dissipation in amplitude-modulation (tapping-mode) force microscop*y. Physical Review B **64**, 193411 (2001)

FIGURE CAPTIONS

Figure 1. Schematic top view of the sensor structure. The small fingers at the end of the cantilever will constitute the electrodes for the electrochemical current detection (separation between them less than 50 nm)

Figure 2. Schematic illustration of the sensor (cantilever with two finger-electrodes). a) Sensor in rest position, b) the cantilever bending is due to the induced surface stress caused by the attachment of small masses.

Figure 3. Schematic diagram of the implemented electrodes at the free end of each cantilever to allow the electrochemical current detection

Figure 4. SEM image of the cantilever and the cavity obtained from the back side of the wafer

Figure 5: Processing sequence to define the electrodes gap using AFM lithography. (a) Deposition of 8 nm Al layers on front (lithography mask) and back (protection mask) sides of the wafer. (b) Local oxidation of Al with AFM to define the 20-100 nm electrode gaps. (c) Selective etching of Al_2O_3. (d) Reactive Ion Etching to fabricate the electrode gaps. (e) Etching of Al layers used as mask on the front side and as protection on the back side.

Figure 6: AFM images of the line defined with AFM lithography. (a) After AFM local oxidation of Al. (b) Same line after selective etching of the Al_2O_3.

Figure 7. a) SEM image of the end of the cantilever structure shown in figure 3c after AFM lithography and partial dry etching; in circles the separation lines for defining the electrodes. b) Detailed SEM image of one of the separation lines. The width is less than 50 nm.

Figure 8. SEM Images of the structure after RIE definition of the nanometric gaps between electrodes. (a) The electrodes are still bonded by the Al on the back side. (b) The two electrodes in a) have been separated by pressing with the AFM tip. (c) Top view of the completed released cantilever.

Figure 9: Images of the AFM tip on the cantilever surface while pressing down for breaking the Aluminum layer (a) and same area with the AFM far from the cantilever surface (b) (Dimensions in μm).

Table 1. Dimensions of some implemented silicon cantilevers to define the sensors (for silicon layer thickness of 0.8 μm, 1.3μm, 1.5μm and 1.8μm). The dimensions of the cantilevers have been adjusted for spring constants around 20 pN/nm and taking into account the dispersion on the nominal value of the cantilever thickness (1,3± 0,5 μm).

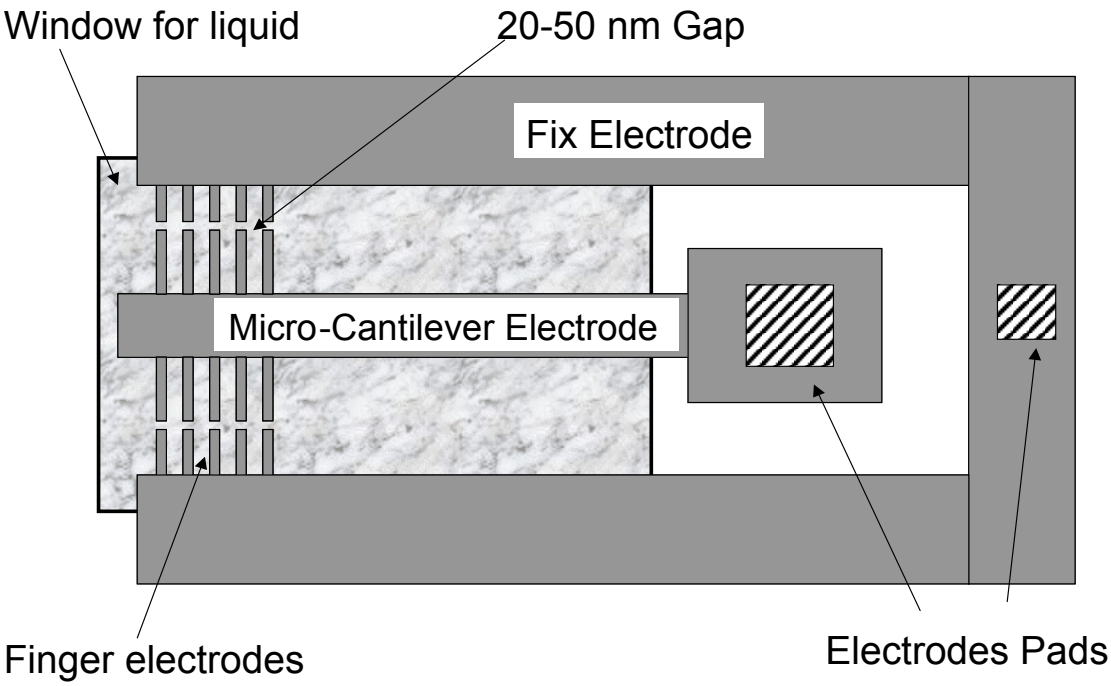

FIG 1. M.Villarroya et al.

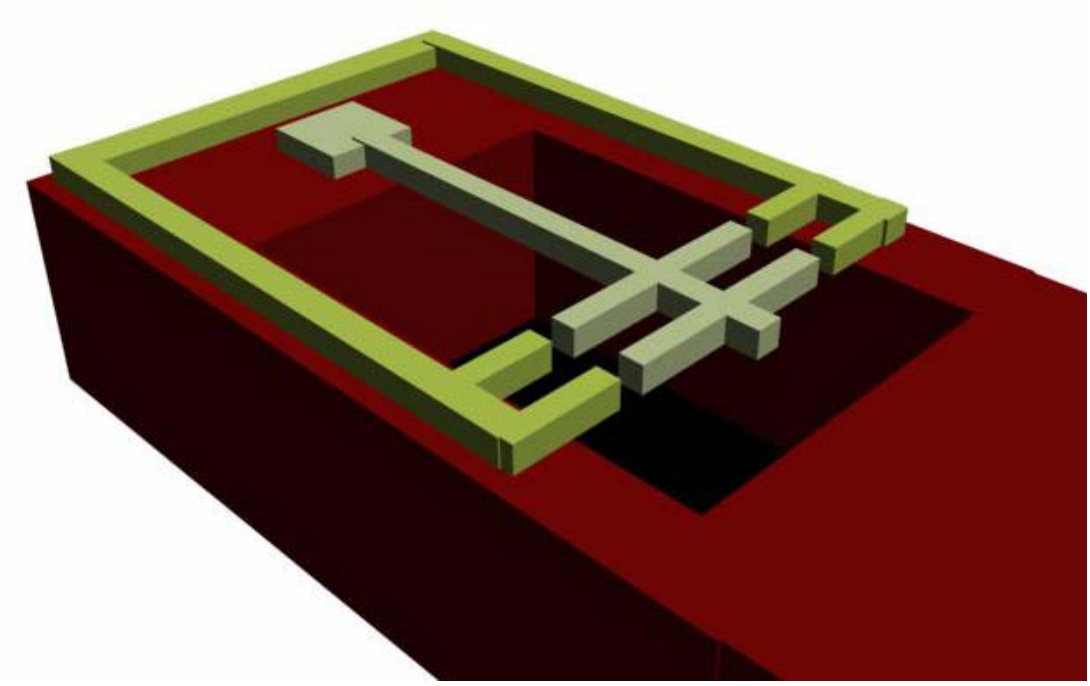

A) Cantilever in rest

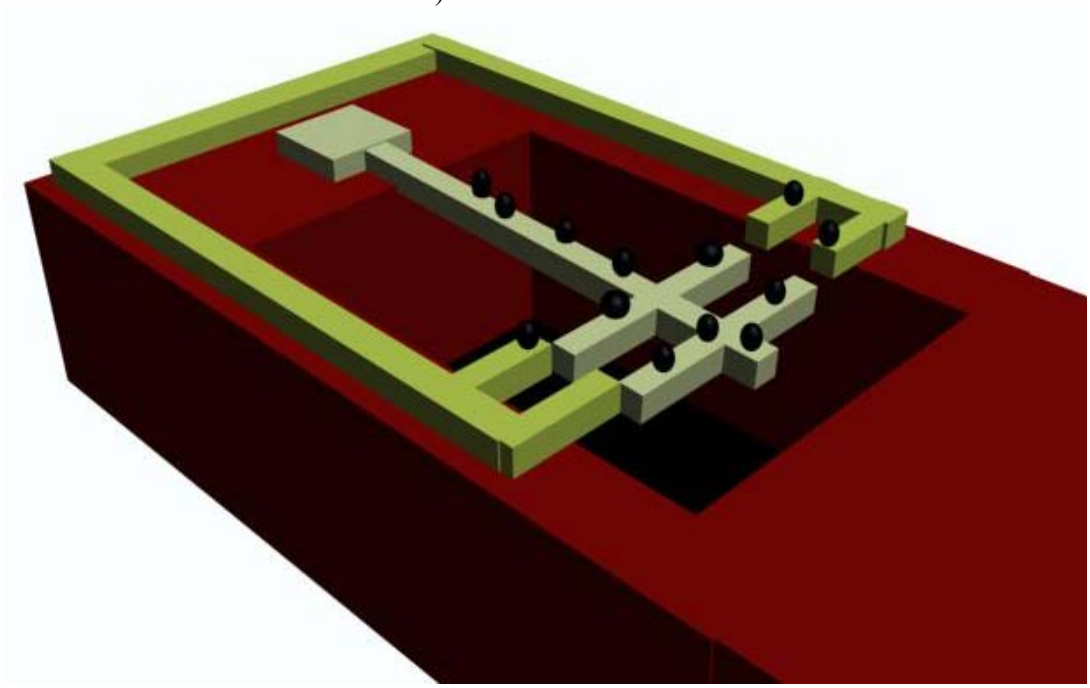

B) Cantilever deflected

FIG 2. M.Villarroya et al.

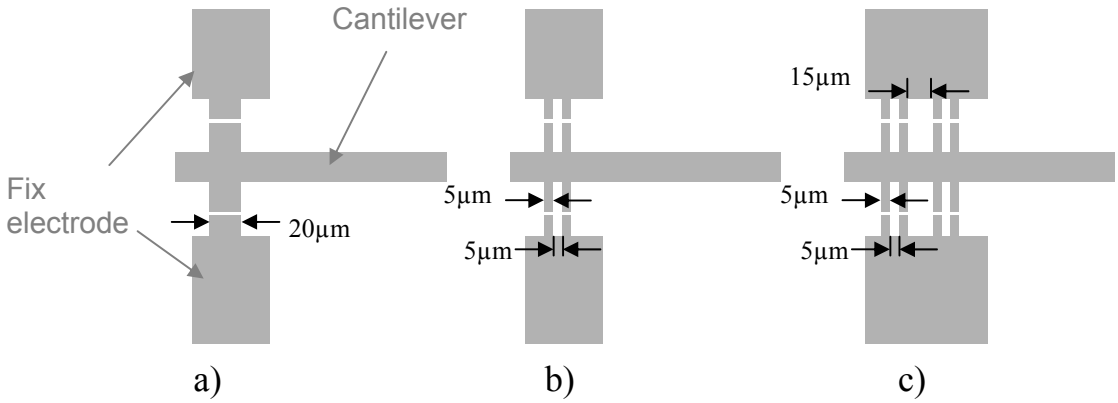

FIG 3. M.Villarroya et al.

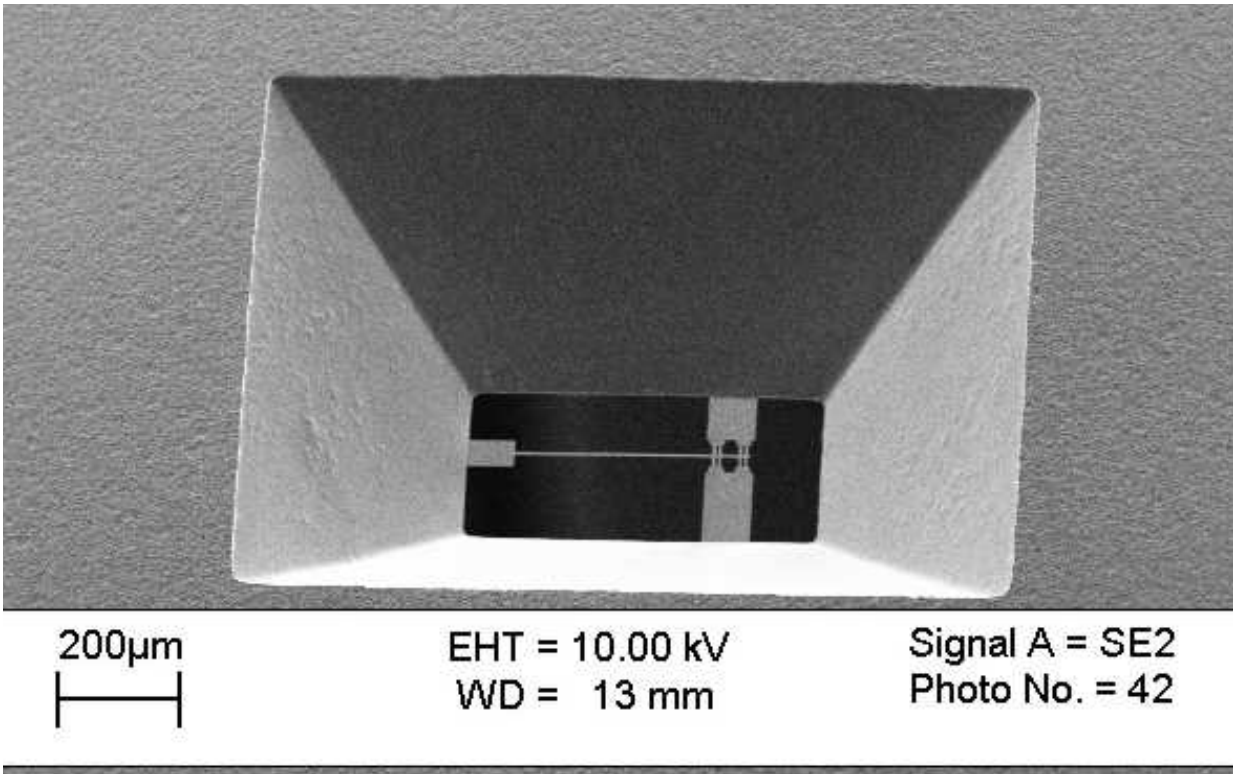

FIG 4. M.Villarroya et al.

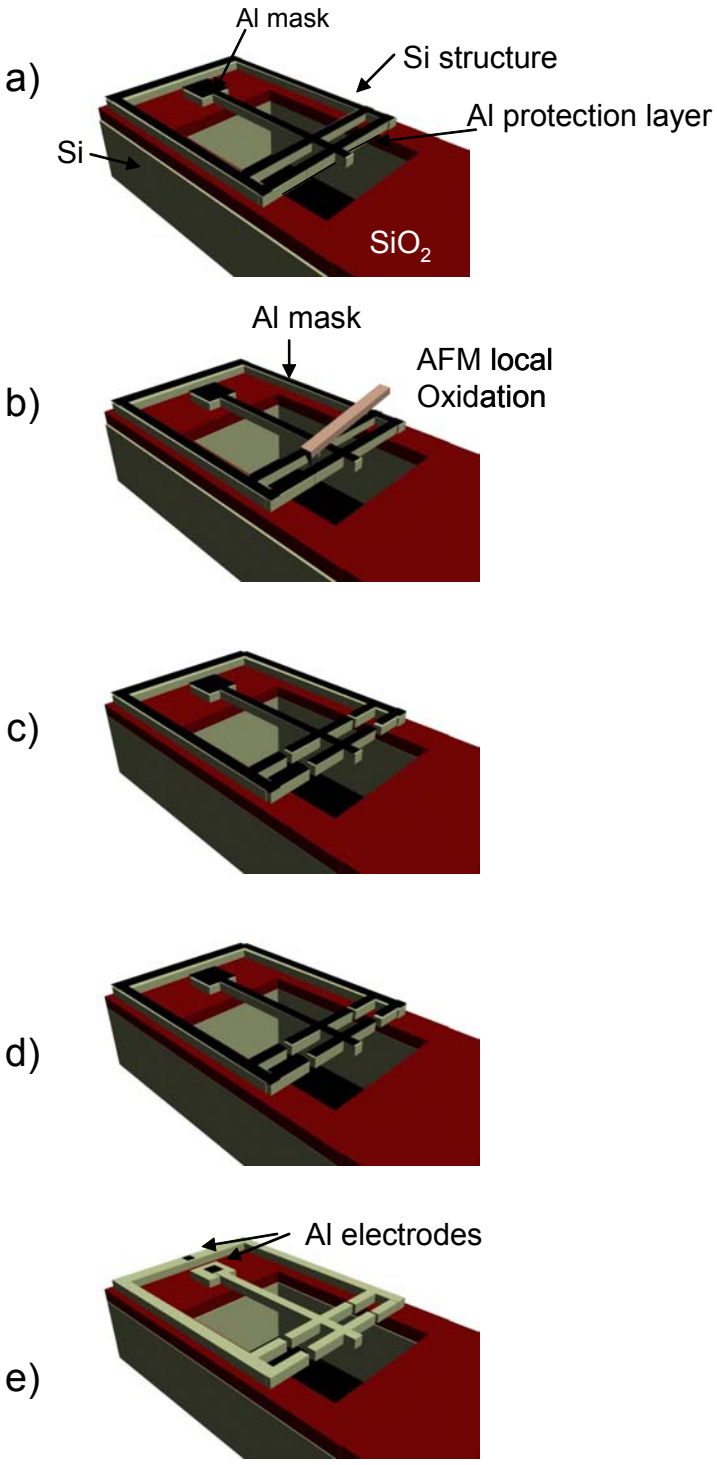

Figure 5. M. Villarroya et Al.

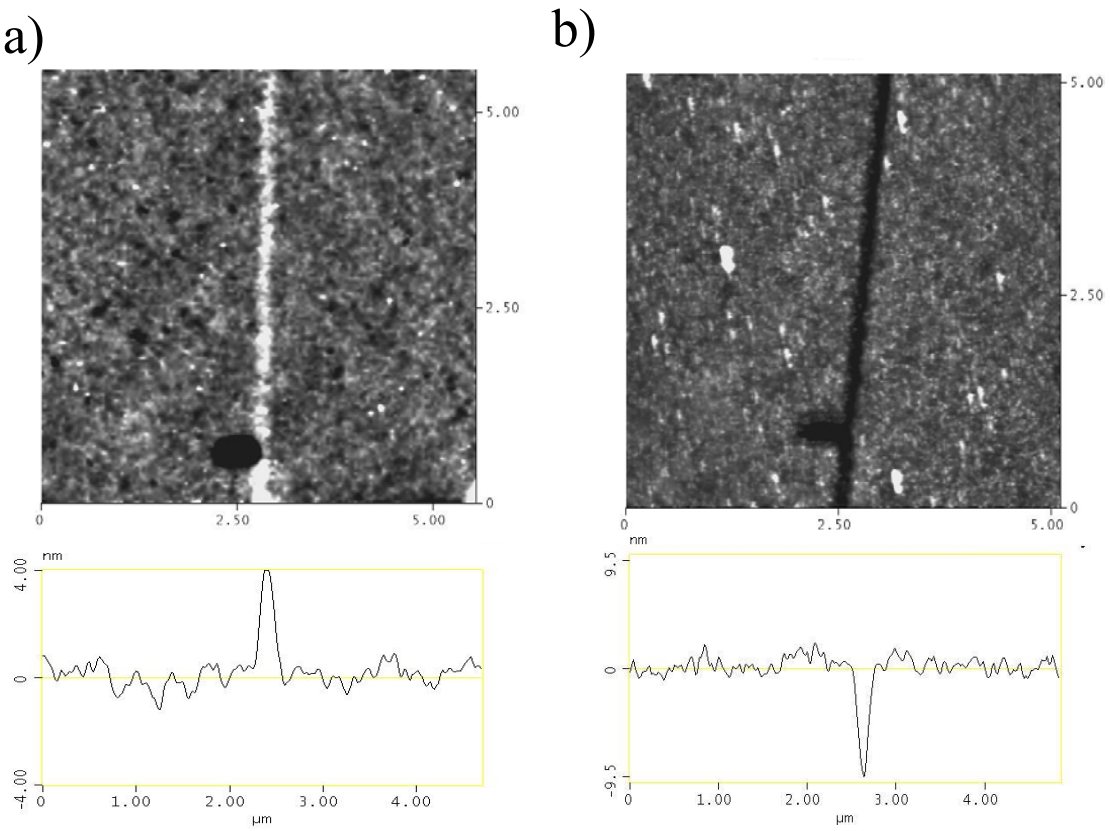

Figure 6. M.Villarroya et Al

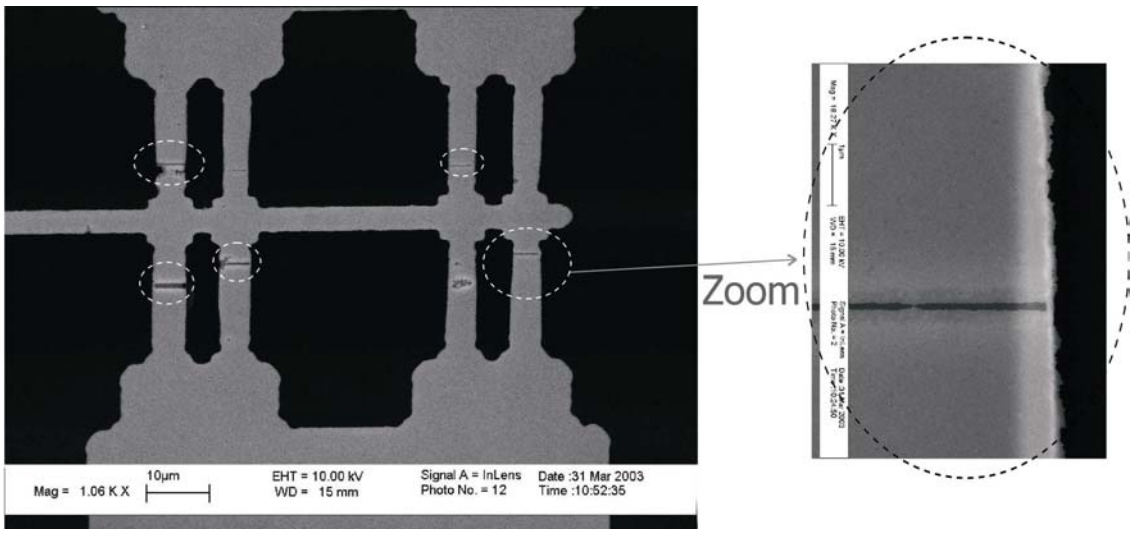

Figure 7. M.Villarroya et al.

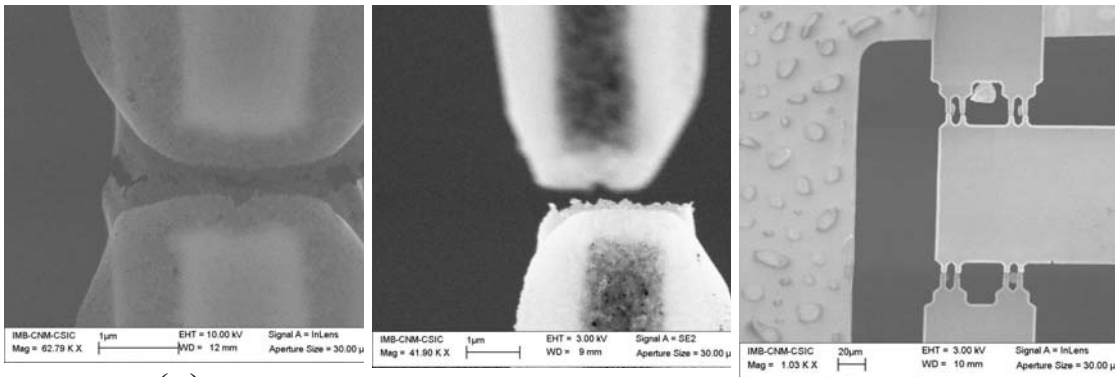

(a) (b) (c)

Figure 8. M.Villarroya et Al

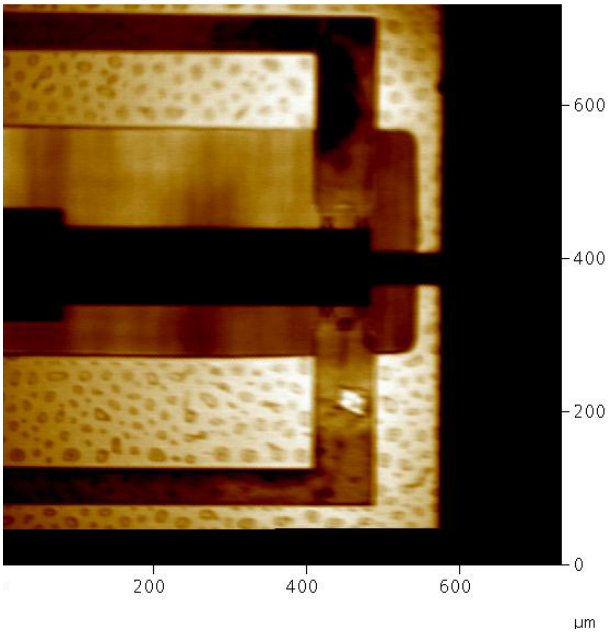

a)

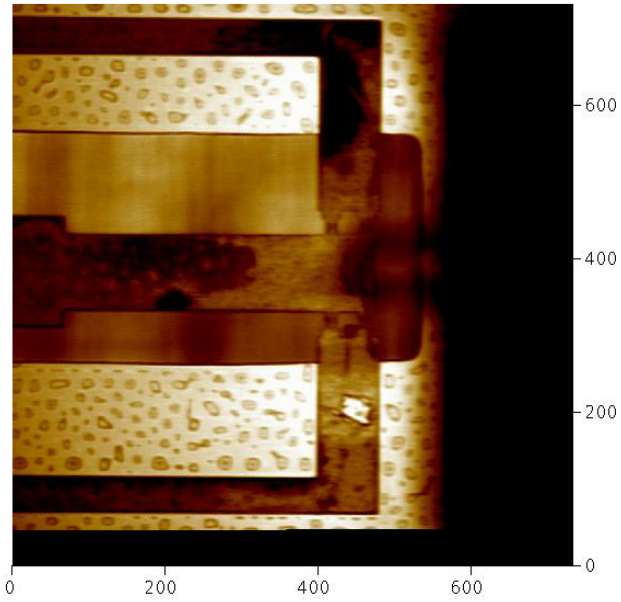

b)

Figure 9. M. Villarroya et Al

Cantilever Length µm	Cantilever Width µm	Spring constant (pN/nm) for different thickness (t)			
		k1 (t=0.8 µm)	k2 (t=1.3µm)	k3 (t=1.5µm)	k4 (t=1.8µm)
400	12	4.32	18.54	28.48	49.21
400	36	12.96	55.61	85.43	147.62
500	25	4.61	19.77	30.38	52.49
500	75	13.82	59.32	91.13	157.46
600	44	4.69	20.14	30.94	53.46
600	130	13.87	59.50	91.41	157.95

TABLE 1. M.Villarroya et al.